

## Design and Analysis of Fusion Algorithm for Multi-Frame Super-Resolution Image Reconstruction using Framelet

K. Joseph Abraham Sundar<sup>\*,!</sup>, V. Vaithyanathan<sup>\*</sup>,  
G. Raja Singh Thangadurai<sup>#</sup> and Naveen Namdeo<sup>#</sup>

<sup>\*</sup>*School of Computing, SASTRA University, Thanjavur - 613 401, India*

<sup>#</sup>*Defence Research and Development Laboratory, Hyderabad - 500 058, India*

<sup>!</sup>*E-mail: joseph@sastra.ac.in*

### ABSTRACT

A enhanced fusion algorithm for generating a super resolution image from a sequence of low-resolution images captured from identical scene apparently a video, based on framelet have been designed and analyzed. In this paper an improved analytical method of image registration is used which integrates nearest neighbor method and gradient method. Comparing to Discrete Wavelet Transform (DWT) the Framelet Transform (FrT) have tight frame filter bank that offers symmetry and permits shift in invariance. Therefore using framelet this paper also present a framelet based enhanced fusion for choosing the fused framelet co-efficient that provides detailed edges and good spatial information with adequate de-noising. The proposed algorithm also has high advantage and computationally fast which are most needed for satellite imaging, medical imaging diagnosis, military surveillance, remote sensing etc.

**Keywords:** Framelet, super resolution, image registration, tight frames

### 1. INTRODUCTION

In any image-capturing system, the quality of the acquired image depends on many variants. One such variant is motion blur due to the movement of the capturing platform against the earth motion, atmospheric distortion, and so on, which affects the quality of the image considerably. One of the low-cost methods to resolve this issue is the software-based signal processing which can eliminate the blur in the captured image and also can get back spatial frequency information above the diffraction cap of the optical system<sup>1</sup>.

Super resolution (SR) image may be defined as a constructed higher resolution (HR) image by combining group of lower resolution images that are sub-pixel altered from one another. The sub-pixel shifted images are usually affected by blur, noise, etc. Every low-resolution image will have additional information concerning about the scene. By grouping or super embossing many low-resolution images of particular scene, a single high resolution image can be constructed. By doing this all the additional information of every low-resolution image is on a single HR image which becomes a SR image, thus fusion of low-resolution images increases the resolution.

One of the predominant methods for super resolution image construction is frequency domain method<sup>2</sup>. The basic concept of frequency domain approach is to consider the low-resolution images in frequency domain as aliased signal, and to find out the de-aliased signal which is the HR image. In the frequency domain method, several restrictions are set on the observation model. Further construction needs prior knowledge of the data and also a laborious process since data is inter-correlated in frequency domain.

Second method is projection on to convex sets<sup>2</sup>. The HR image is acquired by introducing a cost function based on linear model defining the relevance between the HR and low-resolution images. But the use of linear model results in non-uniqueness of the solution and high computation.

Third method is statistical method for SR image reconstruction based on Bayesian method<sup>3</sup> which uses maximum probability to find the solution. This method castigates the edge information and thereby reducing the quality of HR image. Recent decades have shown many reconstruction methods in spatial domain including the iterative back projection approach<sup>4</sup>, maximum likelihood approach<sup>5</sup>, maximum *a posteriori* (MAP) approach<sup>6,7</sup>, hybrid approach<sup>8</sup>, etc.

The recent advancement for SR image is the use of wavelet transformation<sup>9,10</sup>. Wavelets were first introduced as the base of a powerful new path to image analysis called multi-resolution theory. As the name indicates, multi resolution theory is involved with the analysis of images at more than one resolution. It uses the inverse wavelet transform for combining low-resolution images that are subjected to various levels of decomposition to produce a HR image. Generally, wavelets have less spatial information and these do not have symmetry, except in Haar wavelet.

The recent decades have made use of framelet for image inpainting which is the fundamental problem in image processing<sup>11</sup>. Based on tight framelet digital image, watermarking has also been developed in the recent years<sup>12</sup>. The proposed method of enhanced fusion using framelet provides symmetry and preserves the edge information, providing a fruitful solution for numerous realistic cases.

## 2. MATHEMATICAL FORMULATION FOR SUPER RESOLUTION IMAGE

Super resolution image reconstruction plays an important role in remote sensing as the satellite images are of multi-phase, multi-platform, multi-spectral and multi-sensor. In such remote sensing applications, ample image data are of taken from same area. To begin with, examine the super resolution image reconstruction problem and develop a perception model that correlates the original high resolution image to the observed low-resolution images.

Let the HR image is of size  $P_1Q_1 \times P_2Q_2$  taken in vector format as  $X = [x_1, x_2, \dots, x_N]^T$ , where  $N = P_1Q_1 \times P_2Q_2$ . The  $i^{th}$  lower resolution image be denoted in the vector form as  $y_i = [y_{j,1}, y_{j,2}, \dots, y_{j,M}]^T$  for  $j = 1, 2, \dots, p$  and  $M = Q_1 \times Q_2$ . The problem formulation is given by<sup>13,14</sup>

$$y_i = DB_iW_iX + n_i \quad (1)$$

where  $y_i$  - observed low-resolution image,

$D$  - sub sampling matrix,

$B_i$  - blur matrix,

$W_i$  - wrap matrix,

$X$  - original HR image,

$n_i$  - noise.

In practical cases, the wrap matrix is considered as the scene is wrapped because of the proportionate motion between the scene and the camera. The image is also degraded by other factors like optical blur, motion blur, and aliasing. So, such factors are taken into consideration for the super resolution image observation model.

## 3. FRAMELET TIGHT FRAME CONDITION AND FILTER BANKS

Wavelets have one scaling and one wavelet function whereas in the case of framelet, it has one scaling function  $\phi(t)$  and two wavelet functions  $\psi_1(t)$  and  $\psi_2(t)$ <sup>15</sup>.

A low-pass filter  $h_0(n)$ , and two high-pass filters  $h_1(n)$  and  $h_2(n)$  are used in defining the scaling function and wavelet function. The scaling function and wavelet function equations are given as :

$$\phi(t) = \sqrt{2} \sum_n h_0(n) \phi(2t - n) \quad (2)$$

$$\psi_i(t) = \sqrt{2} \sum_n h_i(n) \phi(2t - n) \quad i = 1, 2, \dots$$

where  $h_i(n), n \in Z$  are all filters having three-channel filter bank.

Consider  $\phi_k(t) = \phi(t - k)$  and  $\psi_{i,j,k}(t) = \psi_i(2^j t - k)$  for  $i = 1, 2, \dots$   $\phi(t)$  and  $\psi_i(t)$  for which any square integral signal  $f(t)$  is given by<sup>16</sup>

$$f(t) = \sum_{k=-\infty}^{\infty} c(k) \phi_k(t) + \sum_{j=0}^{\infty} \sum_{k=-\infty}^{\infty} d_1(j, k) \psi_{1,j,k}(t) + d_2(j, k) \psi_{2,j,k}(t) \quad (3)$$

where  $c(k) = \int f(t) \phi_k(t) dt$

$$d_i(j, k) = \int f(t) \psi_{i,j,k}(t) dt \quad i = 1, 2.$$

A set of functions  $\{\psi^1, \dots, \psi^{N-1}\}$  in a space,  $L^2$  is named as a frame if and only if  $A > 0, B < \infty$ , so that for any function  $f \in L^2$ ,

$$A \|f\|^2 \leq \sum_{i=1}^{N-1} \sum_j \sum_k \left| \langle f, \psi^i(2^j - k) \rangle \right|^2 \leq B \|f\|^2 \quad (4)$$

where  $A$  and  $B$  are known a frame bounds. Tight frames appears in the special case of  $A=B$ . The bounds  $A$  and  $B$  take on the values given by<sup>17</sup>

$$A = B = \frac{1}{N} \sum_{n=0}^{N-1} \|h_n\|^2 \quad (5)$$

Using scaling function deduce the tight frames, which is common way of using the multi-resolution analysis to have framelet transform.

### 3.1 IDEAL RECONSTRUCTION CONDITIONS

For analysis filter banks, a low-pass filter  $h_0(n)$ , which has an even length and which satisfies the symmetry condition of  $2 - H_0(z)H_0(1/z) - H_0(-z)H_0(-1/z)$  is obtained.

The synthesis filter bank, which is the reconstruction part, was formed by taking the transpose of the analysis filter bank. For this, the analysis filter was time-reversed to produce the synthesis filter. The two equations given below give the criteria for ideal reconstruction based on multi-rate system theory<sup>18,19</sup>

$$\sum_{j=0}^2 H_j(Z)H_j(Z^{-1}) = 2 \quad (6)$$

$$\sum_{j=0}^2 H_j(-Z)H_j(Z^{-1}) = 0$$

The poly-phase components are defined so that

$$H_j(Z) = H_{j_0}(Z^2) + z^{-1}H_{j_1}(Z^2) \text{ for } j = 0, 1, 2. \quad (7)$$

The matrix form of ideal reconstruction is given by the equation

$$H'(Z^{-1})H(Z) = 2I \quad (8)$$

$$\text{where } H(z) = \begin{pmatrix} H_{00}(Z) & H_{01}(Z) \\ H_{10}(Z) & H_{11}(Z) \\ H_{20}(Z) & H_{21}(Z) \end{pmatrix}$$

With  $h_0(n)$  being the low-pass filter which is symmetric,  $h_1(n)$  and  $h_2(n)$  being high-pass filter which are symmetric or anti-symmetric, the objective is to construct three filters fulfilling the ideal reconstruction criteria.

### 3.2 ANALYTICAL METHOD OF IMAGE REGISTRATION

There are numerous algorithms for image registration. Among these the gradient method<sup>20</sup> suits more for practical applications. But it works best in case the shift is small for low-resolution images. To overcome this, integrate the iterative technique<sup>4</sup> with the image registration algorithm<sup>20</sup>. Here, we consider the first frame  $r_i(x, y)$  as the reference image. Considering this as reference the shifts in the remaining frames were calculated. Assume  $X$  denotes the total frames contained in a video,  $p_i$  and  $v_i$  denotes the shifts in horizontal direction and vertical direction, respectively for the  $i^{th}$  frame. The  $i^{th}$  frame can be expressed as

$$r_i(x, y) = r_i(x + p_i, y + v_i) \quad (9)$$

where  $k \in \{2, 3, 4, \dots, X\}$ . By<sup>21</sup> approximating Eqn. (9) we get

$$r_i \approx r_1(x, y) + p_i \frac{\partial r_1(x, y)}{\partial x} + v_i \frac{\partial r_1(x, y)}{\partial y} \quad (10)$$

For solving the parameters  $p_k$  and  $v_k$ , apply the method of least square. For least square solution<sup>22</sup> the error equation

$$E_i(p_i, v_i) \approx \frac{1}{MN} \sum_{m=1}^M \sum_{n=1}^N [r_i(m, n) - r_1(m, n) - p_i \frac{\partial r_1(x, y)}{\partial x} + v_i \frac{\partial r_1(x, y)}{\partial y}]^2 \quad (11)$$

should be minimised,

where  $m$  and  $n$  - discrete variables for  $x$  and  $y$  directions respectively,  $M$  and  $N$  - total number of pixels in  $x$  and  $y$  directions respectively,  $p_i$  and  $v_i$  - are the translational shifts in  $x$  direction and  $y$  direction between  $i^{\text{th}}$  frame and original image.

Way of minimizing is to differentiate Eqn. (11) wrt  $p_i$  and  $v_i$  making the derivative equal to zero. Simultaneously solving the deriving equation, it can be represented as Eqn. (12):

$$\begin{pmatrix} \sum_{m=1}^M \sum_{n=1}^N \left( \frac{\partial r_1(m, n)}{\partial m} \right)^2 & \sum_{m=1}^M \sum_{n=1}^N \left( \frac{\partial r_1(m, n)}{\partial m} \frac{\partial r_1(m, n)}{\partial n} \right) \\ \sum_{m=1}^M \sum_{n=1}^N \left( \frac{\partial r_1(m, n)}{\partial m} \frac{\partial r_1(m, n)}{\partial n} \right) & \sum_{m=1}^M \sum_{n=1}^N \left( \frac{\partial r_1(m, n)}{\partial n} \right)^2 \end{pmatrix} \begin{pmatrix} p_i \\ v_i \end{pmatrix} = \begin{pmatrix} \sum_{m=1}^M \sum_{n=1}^N (r_i(m, n) - r_1(m, n)) \frac{\partial r_1(m, n)}{\partial m} \\ \sum_{m=1}^M \sum_{n=1}^N (r_i(m, n) - r_1(m, n)) \frac{\partial r_1(m, n)}{\partial n} \end{pmatrix} \quad (12)$$

Equation (12) can be written in matrix form as  $R \cdot S = V$

$$\text{where } V = \begin{pmatrix} \sum_{m=1}^M \sum_{n=1}^N (r_i(m, n) - r_1(m, n)) \frac{\partial r_1(m, n)}{\partial m} \\ \sum_{m=1}^M \sum_{n=1}^N (r_i(m, n) - r_1(m, n)) \frac{\partial r_1(m, n)}{\partial n} \end{pmatrix}$$

The registration parameter can be calculated as  $S = R^{-1}V$ . The frame  $r_i(m, n)$  is shifted by using these estimated shifts so that it closely matches with  $r_1(m, n)$ . The procedure is repeated till the registration estimates becomes as small as possible.

#### 4. PROPOSED ALGORITHM

The proposed algorithm consists of the following stages. (i) Image Registration, (ii) Image decomposition based on framelet transform, (iii) Framelet based image fusion. Figure 1 gives the hierarchal flow of the proposed algorithm.

Algorithm for framelet-based enhanced fusion is as follows

- Obtain consecutive frames (low-resolution images) which are shifted and rotated from a video sequence.
- Using analytical method of image registration, register the sub-pixels that are shifted and rotated in the low-resolution images.
- Decompose the registered images into its framelet transform coefficient using 2-D framelet transform
- If a colour image is used, the above steps are to be repeated for R, G, and B bands for the low-resolution color image.

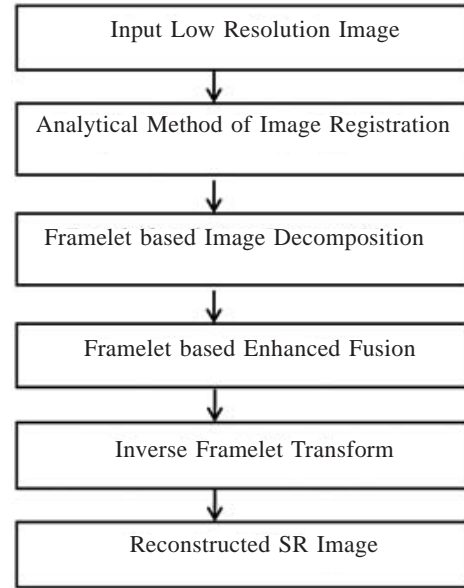


Figure 1. Proposed algorithm flowchart.

- Create a fused framelet transform using framelet-based enhanced fusion.
- Taking inverse framelet transform gives the fused image which is the SR image.

#### 4.1 FRAMELET-BASED DECOMPOSITION

The analysis and synthesis filter banks were used for implementing framelet transform on the images. One low-pass filter  $h_0(n)$  along with two high-pass filters  $h_1(n)$  and  $h_2(n)$  dwell in the analysis filter bank. The analysis filter bank transforms the input image into three sub-bands  $H_0(Z)$ ,  $H_1(Z)$  and  $H_2(Z)$ .

$$H(z) = \sum_n h(n)z^{-n} \text{ denotes } Z\text{-transform of } h(n).$$

Each band is then down sampled by two. These are namely low-frequency sub-band, and two high-frequency sub-bands. The synthesis stage filters and analysis stage filters need not be the same. In this case where image is used, a two dimensional transform is required. A two-dimensional separable transform is similar to two one-dimensional transforms in series. One dimensional row transform succeeded by one-dimensional column transform brings the two-dimensional transform which is shown in Fig. 2. The transform is more efficient under the tight frame condition given in Eqn. (5),  $A = B = \frac{1}{N} \sum_{n=0}^{N-1} \|h_n\|^2$ , where  $A$  and  $B$  are known as frame bounds

#### 4.2 FRAMELET-BASED ENHANCED FUSION

The general practice of obtaining a fused framelet transform is by averaging the framelet coefficients. This leads to the blurring of the edge information and hiding of the finer details. So, much simpler method of creating fused framelet transform is proposed. Using all the registered images, the highest value of the pixel from the framelet transform was selected for creating the fused framelet transform. Let  $a_{ij}$ ,  $b_{ij}$ , and  $c_{ij}$  denote the framelet coefficient of reference frame, and registered frames respectively. Then the, fused framelet

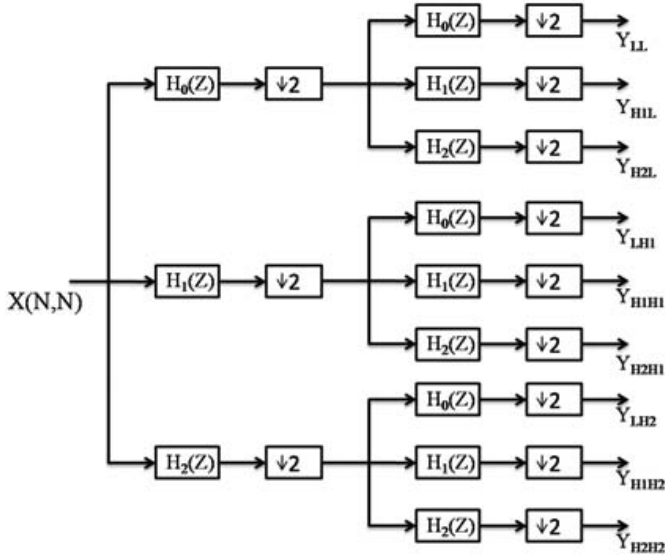


Figure 2. 2-D analysis filter bank.

coefficient  $f_{ij}$  is given by

$$f_{ij} = \begin{cases} a_{ij} & \text{if } a_{ij} > b_{ij} \text{ and } c_{ij} \\ b_{ij} & \text{if } b_{ij} > a_{ij} \text{ and } c_{ij} \\ c_{ij} & \text{if } c_{ij} > a_{ij} \text{ and } b_{ij} \end{cases} \quad (13)$$

where  $i$  and  $j$  denote the rows and columns of images. The inverse framelet transform of this gives the reconstructed super resolution image. Figure 3 gives a better picture of the process.

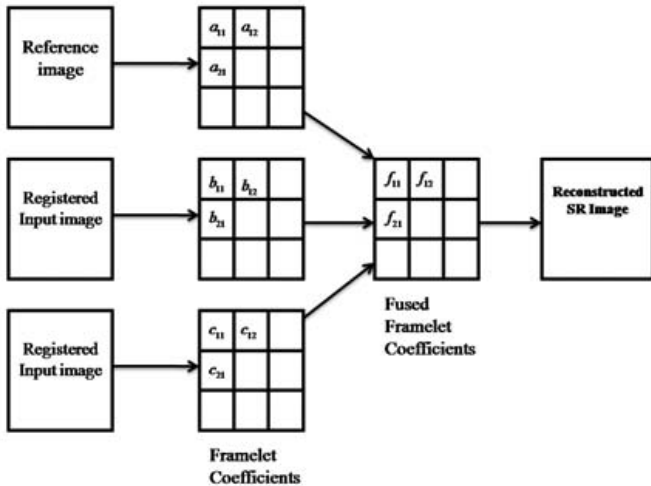


Figure 3. Framelet-based fusion of low-resolution images.

## 5. RESULTS AND DISCUSSIONS

The experimental data and the results of the experiments with various methods and the proposed framelet method are presented in this section along with some analysis and discussions.

### (a) Experimental Setting

For testing the performance of the framelet SR model, five data sets are used. The first three experiments are simulated experiments with known HR image. The next two experiments

are real data experiments where the HR image is not known. In all of these experiments, the analytical method of image registration is assumed. To evaluate the reconstruction results, peak signal-to-noise-ratio (PSNR) and sharpness index<sup>23</sup> are used for the case of stimulated experiments. The original HR image is not known in the case of real data experiments. So the evaluation was done based on blind image quality index (BIQI)<sup>24</sup> and sharpness index<sup>23</sup>. For both of these indices, higher the values, better the image quality. The relative merit of the proposed model is assessed by comparing with the wavelet method and frequency domain method.

### (b) Experimental Results

Initially the image quality index is calculated without the application of super resolution. The values obtained are tabulated in the Table 1 and Table 2.

**Table 1. PSNR and sharpness index values of different images in simulated experiments**

Low-resolution sequence	PSNR	Sharpness index
EIA	17.3318	19.2993
Alpaca	15.2695	14.2359
Disk	18.9267	13.6626

**Table 2. BIQI and sharpness index values of different images in real data experiments**

Low-resolution sequence	BIQI	Sharpness index
Aerial 1	38.3281	14.5374
Aerial 2	11.5911	11.9759

In the simulated experiments, to verify the proposed algorithm, three data sets are taken from Multidimensional Signal Processing Research Group of UCSC<sup>25</sup>. For reducing the complexity, the first four frames from the three data sets are selected. As the number of frames increases, the quality also increases provided a compromise on the computation time is done. A strong registration method discussed in Section 3.2 is used as motion estimation model. Figure 4-6 shows the reconstruction results of these three data sets. In these figures, (a) is one frame of the low-resolution image sequence; (b) is the wavelet method reconstruction result; (c) is the frequency domain reconstruction result; and (d) presents the proposed framelet reconstruction result.

The evaluation results are shown in Table 3. This also shows that the proposed framelet method almost has the highest values of PSNR and sharpness index which is consistent with the visual results presented in Figs. 4-6.

In real data experiments, two data captured by an unmanned aerial vehicle (UAV) used are, respectively, 'Aerial 1' image having 297 uncompressed frames of size 640 x 480 and 'Aerial 2' image having 438 uncompressed frames of size 720 x 480. Figures 7-8 show the reconstruction results of the two real data sets. In these figures, (a) is one frame of the low-resolution image sequence; (b) is the wavelet method reconstruction result; (c) is the frequency domain reconstruction result; and (d) presents the proposed framelet reconstruction result.

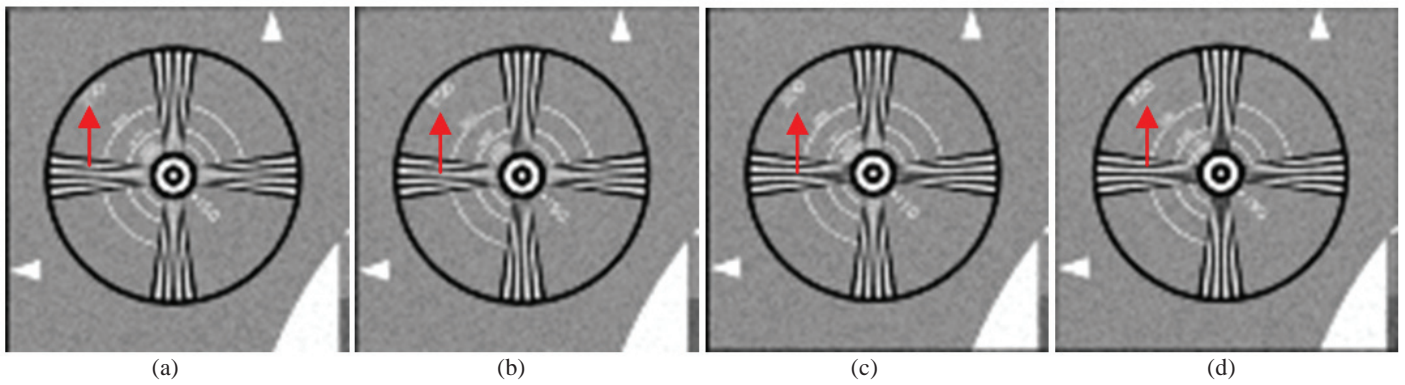


Figure 4. Reconstruction results of the 'EIA' image sequence: (a) low-resolution image, (b) wavelet method, (c) frequency domain method, and (d) framelet method.



Figure 5. Reconstruction results of the 'Alpaca' image sequence: (a) low-resolution image, (b) wavelet method, (c) frequency domain method, and (d) framelet method.

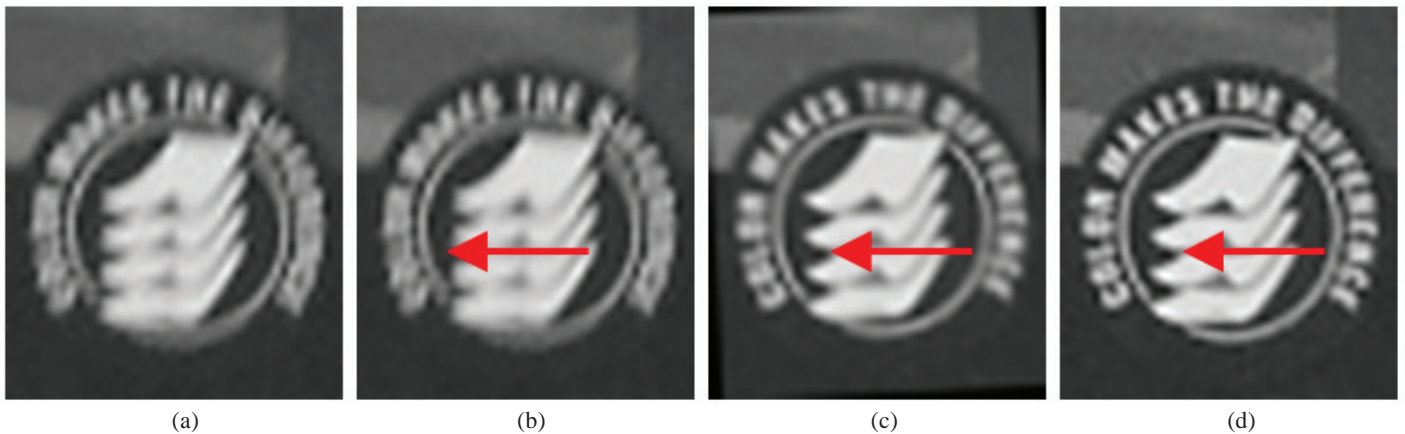


Figure 6. Reconstruction results of the 'Disk' image sequence: (a) low-resolution image, (b) wavelet method, (c) frequency domain method, and (d) framelet method.

Table 3. PSNR and sharpness index values of different reconstruction methods in simulated experiments

Low-resolution sequence	Assessment index	Wavelet method	Frequency domain	Framelet method
EIA	PSNR	31.7238	33.3183	72.5638
	Sharpness Index	21.3025	21.9033	21.9616
Alpaca	PSNR	30.7164	36.2393	57.8823
	Sharpness Index	17.0750	18.7591	18.8157
Disk	PSNR	36.8472	38.4603	55.4846
	Sharpness Index	16.8396	17.9425	19.1814

The good performance of the proposed framelet method is also illustrated by the BIQI and sharpness index tabulated in Table 4. The table shows that the proposed framelet method has the highest values of BIQI and sharpness index, which

Table 4. BIQI and sharpness index values of different reconstruction methods in real data experiments

Low-resolution sequence	Assessment index	Wavelet	Frequency domain	Framelet
Aerial 1	BIQI	43.7090	44.3702	47.5140
	sharpness index	14.1601	15.6753	16.0839
Aerial 2	BIQI	17.9825	18.9845	29.8068
	sharpness index	11.8850	13.7608	13.7619

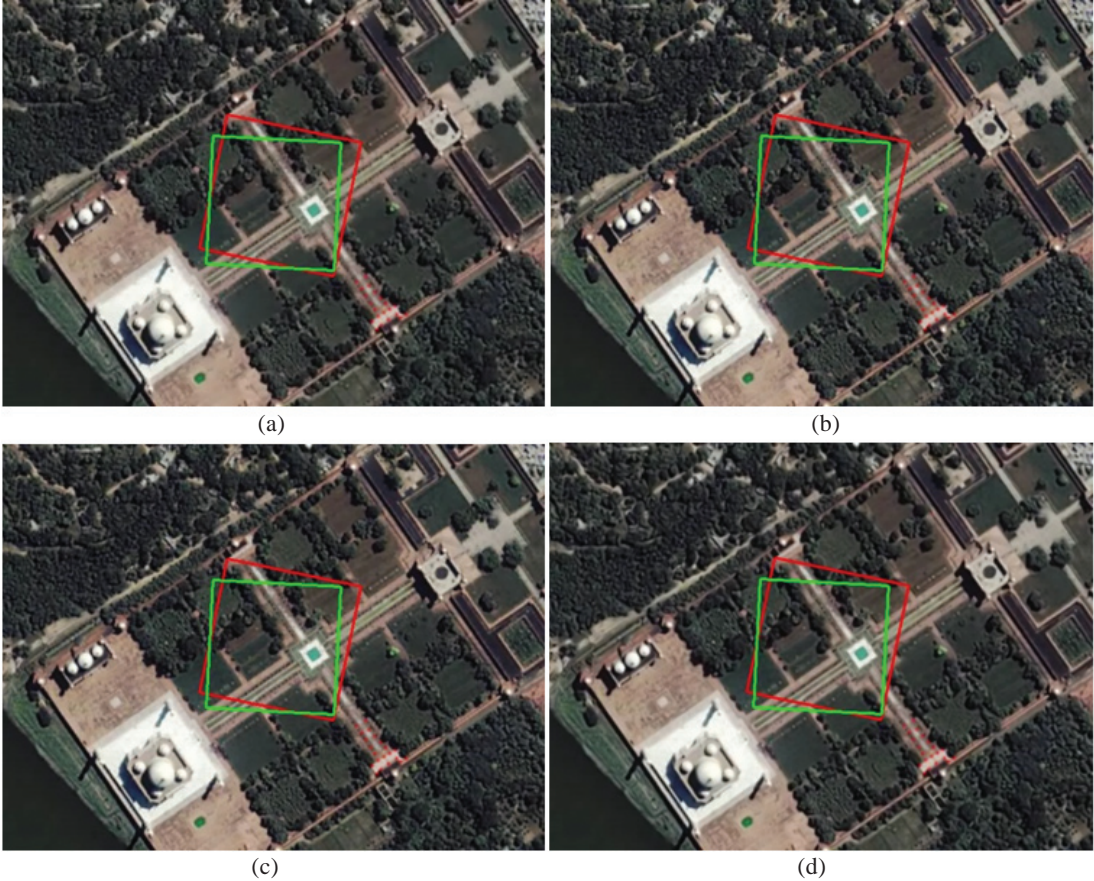


Figure 7. Reconstruction results of the ‘Aerial 1’ image sequence: (a) low-resolution image, (b) wavelet method, (c) frequency domain method, and (d) framelet method.

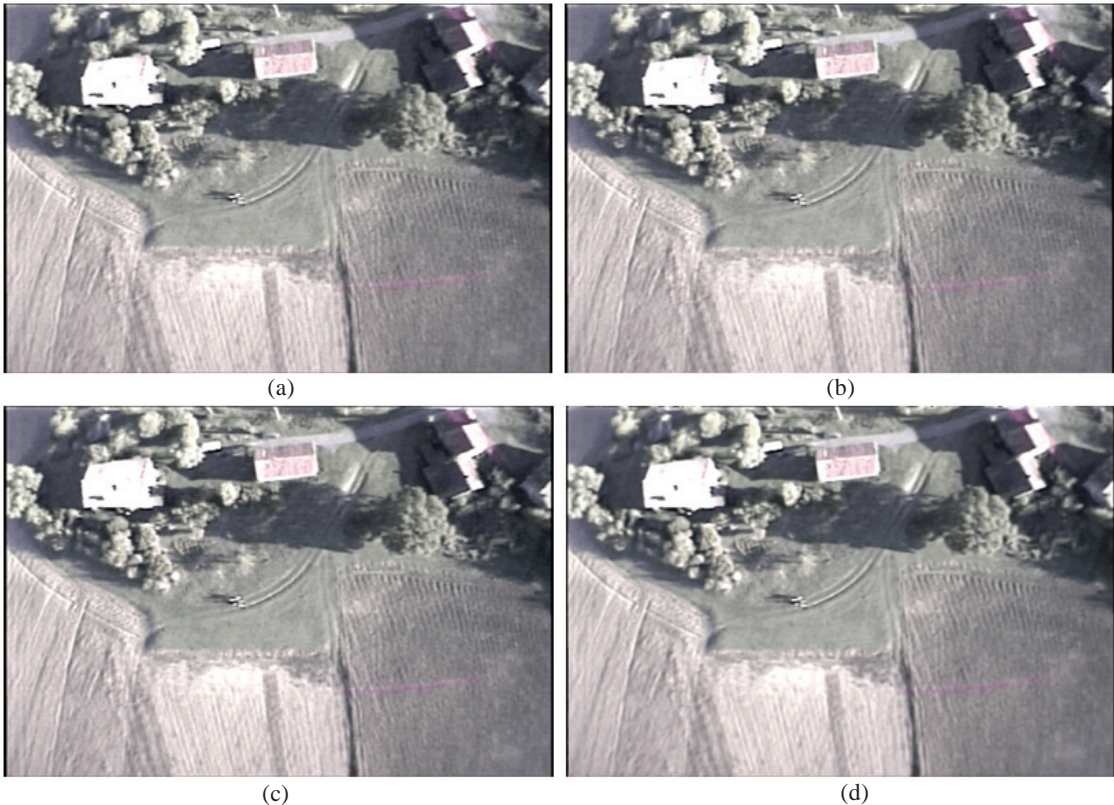


Figure 8. Reconstruction results of the ‘Aerial 2’ image sequence: (a) low-resolution image, (b) wavelet method, (c) frequency domain method, and (d) framelet method.

illustrates that the proposed framelet method produces a better reconstruction result.

### (c) Discussion

Using SR technique, the resolution of the image has increased which is quite evident from the figures. In wavelet result, though the noise is suppressed, some artifacts are produced. In case of frequency domain results the artifacts are reduced to some extent, the edge information is not well preserved. But in framelet method, the noise and artifact is greatly suppressed also preserving the edge information. In Fig. 6, the word 'colour' in the disk sequence is well preserved and can be clearly identified in the framelet method compared to two reconstruction methods. Among the three reconstruction algorithms, the proposed framelet method shows better result. In the smooth areas, the noise is greatly suppressed, and in the edge information is well preserved.

## 6. CONCLUSION

In this paper a framelet-based enhanced fusion for super resolution image reconstruction is proposed. The proposed enhanced fusion process for choosing the fused framelet coefficient helps in retaining adequate features and edges which highly improves the super resolution results. Experimental results presented in Section 5 show that the proposed framelet method suppress the noise, reduces the artifacts, and also preserves the edge information. The discussion and analysis about experiments also illustrate that proposed algorithm is highly advantageous and gives good performance improvement compared to other methods using real time images and video frames.

## REFERENCES

1. Liyakathunisa, L.; Kumar C.N.R. & Ananthashayana, V.K. Super resolution reconstruction of compressed low-resolution images using wavelet lifting schemes. In 2<sup>nd</sup> IEEE International Conference on Computer and Electrical Engineering 2009: Dubai, 2009. doi: 10.1109/ICCEE.2009.221
2. Pandya, Hardeep; Prashant, B. & Swadas, Mahasweta, Joshi. A survey on techniques and challenges in image super resolution reconstruction. *Int. J. Comput. Sci. Mobile Comput.*, 2013, **2**(4), 317 – 325.
3. Derin, Babacan, S.; Rafael, Molina & Aggelos, Katsaggelos. Variational bayesian super resolution. *IEEE Trans Image Process.*, 2011, **20**(4), 984 - 999. doi: 10.1109/tip.2010.2080278
4. Irani, M. & Peleg, S. Improving resolution by image registration. *Comput. Vis. Graph. Image Process.*, 1991, **53**(3), 231–239. doi: 10.1016/1049-9652(91)90045-1
5. Tom, B. & Katsaggelos, A. Reconstruction of a high-resolution image by simultaneous registration, restoration, and interpolation of low-resolution images. In Proceedings of the IEEE International Conference on Image Processing 1995: Washington, 1995. doi: 10.1109/icip.1995.537535
6. Schultz, R. & Stevenson, R. Extraction of high-resolution frames from video sequences. *IEEE Trans. Image Process.*, 1996, **5**(6), 996–1011. doi: 10.1109/83.503915
7. Belekos, S.; Galatsanos, N. & Katsaggelos, A. Maximum *a posteriori* video super-resolution using a new multichannel image prior. *IEEE Trans. Image Process.*, 2010, **19**(6), 1451–1464. doi: 10.1109/TIP.2010.2042115
8. Elad, M. & Feuer, A. Restoration of a single super resolution image from several blurred, noisy, and under sampled measured images. *IEEE Trans. Image Process.*, 1997, **6**(12), 1646–1658. doi: 10.1109/83.650118
9. Nguyen, N. & Milanfar, P. A wavelet-based interpolation restoration method for super resolution (wavelet super resolution). *Circuits Syst. Signal Process.*, 2000, **19**(2), 321–338. doi: 10.1007/BF01200891
10. Hui, J. & Fermuller, C. Robust wavelet-based super-resolution reconstruction: Theory and algorithm. *IEEE Trans. Pattern Anal. Mach. Intell.*, 2009, **31**(4), 649–660. doi: 10.1109/TPAMI.2008.103
11. Jian-Feng, Cai.; Raymond, H. Chan. & Zuowei, Shen. A framelet-based image in painting algorithm. *Appl. Comput. Harmon. Anal.*, 2008, **24**(2), 131–149. doi: 10.1016/j.acha.2007.10.002
12. Runhai, Jiao. A digital image watermarking method based on tight framelet. In IEEE International Conference on Web Information Systems and Mining (WISM) 2010: Sanya, 2010. doi: 10.1109/wism.2010.86
13. Jing, Tian. & Kai-Kuang, Ma. Stochastic super-resolution image reconstruction. *J. Vis. Commun. Image R.*, 2010, **21**(3), 232–244. doi: 10.1016/j.jvcir.2010.01.001
14. Jian, Lu.; Hong, Ran, Zhang & Yi, Sun. Video super resolution based on non-local regularization and reliable motion estimation. *Signal Process. Image Commun.*, 2014, **29**(4), 514–529. doi: 10.1016/j.image.2014.01.002
15. Soman, K.P. & Ramamchandran, K.I. Insight into wavelets: from theory to practice. Prentice Hall, India, 2006.
16. Farras, Abdelnour, A. Wavelet design using grobner basis methods. Polytechnic University, Brooklyn, USA, 2002. PhD Thesis.
17. Selesnick, I.W. & Abdelnou, A.F. Symmetric wavelet tight frame with two generators. *Appl. Comput. Harmon. Anal.*, 2004, **17**(2), 211-225. doi: 10.1016/j.acha.2004.05.003
18. Selesnick, I.W. Smooth wavelet tight frames with zero moments. *Appl. Comput. Harmon. Anal.*, 2001, **10**(2), 163-181. doi: 10.1006/acha.2000.0332
19. Hadeeel, N.A. & Taai. A novel fast computing method for framelet coefficients. *Am. J. Appl. Sci.*, 2008, **5**(11) 1522-1527.

- doi: 10.3844/ajassp.2008.1522.1527
20. Schaum & McHugh, M. Analytic methods of image registration: Displacement estimation and resampling. Naval Research Laboratory, User Report No. 9298. Febuary 1992.
  21. Hiep, Luong; Bart, Goossens; Aleksandra, Pizurica & Wilfried, Philips. Total least square kernel regression. *J. Vis. Commun. Image R.*, 2014, **23**(1), 94–99.  
doi: 10.1016/j.jvcir.2011.09.002
  22. Goodman, J.W. Introduction to Fourier optics. McGraw Hill, New York, 1996.
  23. Christoph, Feichtenhofer; Hannes, Fassold & Peter, Schallauer. A perceptual image sharpness metric based on local edge gradient analysis. *IEEE Signal Process. Lett.*, 2013, **20**(4), 379-382.  
doi: 10.1109/LSP.2013.2248711
  24. Moorthy & Bovik, A. A two-step framework for constructing blind image quality indices. *IEEE Signal Process. Lett.*, 2010, **17**(5), 213-216.  
doi: 10.1109/lsp.2010.2043888
  25. Milanfar, P. MDSP Super-resolution and demosaicing datasets. Available: <http://users.soe.ucsc.edu/~milanfar/software/srdatasets.html> [Accessed on 19 November 2014].

## CONTRIBUTORS

**Mr K. Joseph Abraham Sundar** obtained his M Tech (Remote Sensing and Wireless Sensor Networks) from Amrita University, in 2012. He is currently working as Research Scholar in the School of Computing, SASTRA University, Thanjavur. His current research interests include: Pattern recognition and image processing.

In the current study K. Joseph Abraham Sundar has contributed in the concept and design in the aspect of framelet being used towards super-resolution. The coding and the implementation of the ideas were also carried out by him.

**Dr V. Vaithyanathan** obtained PhD from Alagappa University, Karaikudi, in 2004. Presently, he is working as Associate Dean-Research, SASTRA University, Thanjavur. He is also a chair professor of Cognizant Technology Solutions. He has published and presented more than 80 Technical papers in the International /National Journals and Conferences. He has successfully completed seven projects from government organizations such as DRDL, ISRO and NIOT. His current research interests include: Image processing, pattern recognition and cloud computing.

In the current study Dr V. Vaithyanathan has done data analysis. The experimental results were analyzed, interpreted and evaluated by him time to time so as to improve the results.

**Dr G. Raja Singh Thangadurai** obtained his ME (Aero Engg) and PhD (MechEngg) from the Indian Institute of Science (IISc), Bangalore, in 1991 and the Indian Institute of Technology (IIT) Madras, Chennai, in 2004, respectively. Presently, he is working as Scientist G at the Defence Research & Development Laboratory (DRDL), Hyderabad. He is involved in the development of liquid propellant rocket engines and reaction control systems for Prithvi and Agni missiles. He has contributed 10 papers in national journals and conferences. His areas of research are rocket and ramjet propulsion, numerical simulation of internal flows, and supersonic air intakes.

In the current study Dr G. Raja Singh Thangadurai has contribution in the real time experiments which was done using UAV videos was a result of his idea towards defence application.

**Mr Naveen Namdeo** obtained his BE (Elect. Comm. Engg.) from RGPV Technical University, Bhopal, in 2002 and M.Tech (Communication and Signal Processing) from IIT Bombay, in 2010. He joined DRDO as Scientist in the year 2003 and since then he is working DRDL Hyderabad. He is Associate Member of Institute of Electronics and Telecommunication Engineers and Member of Society for Aerospace Quality and Reliability. He has been working in the field of GPS, Software V&V, communication networks and image processing.

In the current study Naveen Namdeo has brought out the significance of the work in the paper clearly. He has revised the paper critically to bring out the intellectual contents. He has also contributed in the analysis and interpretation of the data.